

Exchange bias induced by domain walls in BiFeO₃

K. L. Livesey*

*School of Physics M013, University of Western Australia, 35 Stirling Hwy, Crawley, Western Australia 6009, Australia
and Center for Magnetism and Magnetic Nanostructures, University of Colorado at Colorado Springs,**Colorado Springs, Colorado 80918, USA*

(Received 21 July 2010; published 9 August 2010)

Recent experiments have measured exchange bias in ferromagnetic/BiFeO₃ systems. Bias strength scales with the length of 109° ferroelectric domain walls in the multiferroic BiFeO₃ and only a small training effect is observed. In this paper these unusual behaviors are partly accounted for using a one dimensional phenomenological Landau model. It is shown that antiferromagnetic domain walls may be pinned by ferroelectric domain walls in BiFeO₃ due to magnetoelectric coupling in the model and may have a net moment due to Dzyaloshinskii-Moriya interaction. Therefore there is a pinned net magnetic moment that can give rise to exchange bias. For Co/BiFeO₃, bias is calculated as a function of temperature and domain-wall density and matches well with experiment.

DOI: [10.1103/PhysRevB.82.064408](https://doi.org/10.1103/PhysRevB.82.064408)

PACS number(s): 75.70.Cn, 75.50.Ee, 75.60.Ch, 75.85.+t

I. INTRODUCTION

Exchange bias (a shift in the hysteresis loop) in various ferromagnets (NiFe, CoFeB) has been experimentally demonstrated when those materials are exchange-coupled to ferroelectric and antiferromagnetic (multiferroic) BiFeO₃.^{1,2} The potential to manipulate magnetic bias using an electric field³ is very exciting for technological applications, such as in the design of new memories,⁴ especially at room temperature. However, the mechanism by which exchange bias arises in multiferroic structures is still not well understood and therefore the design of multifunctional devices utilizing this effect is limited. Also, the exchange bias behavior appears to be different from that seen in traditional ferromagnetic/antiferromagnetic systems. Firstly, no training effect has been measured on short time scales;² the bias strength does not decrease on consecutive cycling of the applied field. Secondly, there is experimental evidence that the bias strength scales with the total length of 109° *ferroelectric* domain walls in the BiFeO₃.⁵

In this paper a phenomenological model that partly accounts for these puzzling observations is presented. It is proposed that antiferromagnetic (AFM) domain walls in BiFeO₃ are pinned by ferroelectric (FE) domain walls via magnetoelectric coupling. Such pinning was first seen in YMnO₃ (Ref. 6) with FE domain walls necessarily coinciding with AFM domain walls. It is also shown that AFM domain walls in our model for BiFeO₃ carry a net magnetic moment due to a Dzyaloshinskii-Moriya (DM) interaction (weak ferromagnetism).^{7,8} This means there is a pinned net moment in multiferroic BiFeO₃ that causes bias in the attached ferromagnet (FM). For reasonable estimates of the material parameters in BiFeO₃, it will be shown that the bias in the model matches very well with that measured in experiment. AFM domain walls have previously been identified as possible sources of uncompensated spins giving rise to exchange bias, for example, see Ref. 9.

It should be noted that recently an alternative mechanism was put forward to explain exchange bias at perovskite/perovskite multiferroic interfaces¹⁰ which is more general

than the one described here. That mechanism relies on assumption of a perfect interface with oxygen atoms mediating superexchange between the FM and AFM ions and therefore may not be useful for rougher interfaces or for metal/oxide structures. Moreover, it cannot account for why exchange bias strength scales with the length of FE domain walls in BiFeO₃.

In Sec. II a one-dimensional (1D) phenomenological model for BiFeO₃ is presented and the domain-wall pinning is demonstrated. Also, the DM interaction is shown to lead to a possible net magnetic moment in a sample that has equal volumes of the two different AFM domains. In Sec. III the model is extended to treat a FM/BiFeO₃ interface and exchange bias is calculated. In Sec. IV the results are summarized and the elements lacking in the model are highlighted.

II. DOMAIN-WALL PINNING IN BiFeO₃

A 1D Landau theory is used to model the BiFeO₃ system in order to demonstrate the pinning of AFM and FE domain walls. This model is similar to that used by Daraktchiev *et al.*^{11,12} for a paramagnet with a FE domain wall present. In Ref. 12 these authors also studied the effect that an isolated FE domain wall has on the weak magnetic moment within an AFM domain in BiFeO₃. However, they did not look at the idea of coupled AFM and FE walls as is done here. Moreover, the AFM was treated as a weak ferromagnet with a single order parameter M in Ref. 12, rather than being treated using a two sublattice model such as that described below.

The FE polarization is assumed to lie along a single axis and so can be represented by a scalar P . This simplifies the model considerably but means that only so-called 180° FE domain walls can exist, which separate domains with polarization P along the same axis but in opposite directions. Thus we cannot account for the experimental observation that only 109° FE domain walls, and not 180° or 71° FE domain walls, lead to bias.⁵ This represents an interesting three-dimensional microscopic problem for future work

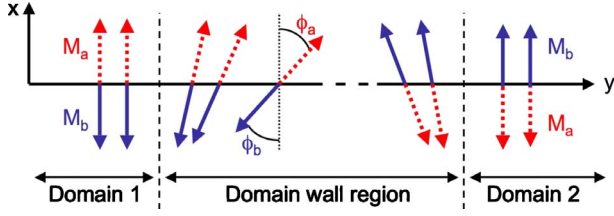


FIG. 1. (Color online) Schematic of the AFM domain wall geometry. The AFM sublattice magnetizations rotate in the x - y plane. The weak DM canting is not visible.

which is outside the scope of the phenomenological 1D model presented here.

The free energy of the multiferroic material is written as a continuous integral over position y

$$F = \int dy \left\{ (K + kP^2)(m_a^2 \sin^2 \phi_a + m_b^2 \sin^2 \phi_b) - bM(m_a \cos \phi_a + m_b \cos \phi_b) + Jm_a m_b \cos(\phi_a - \phi_b) + \frac{1}{2}(C + cP^2) \left[m_a^2 \left(\frac{\partial \phi_a}{\partial y} \right)^2 + m_b^2 \left(\frac{\partial \phi_b}{\partial y} \right)^2 \right] + Dm_a m_b \sin(\phi_a - \phi_b) - \frac{\alpha}{2} P^2 + \frac{\beta}{4} P^4 + \frac{\kappa}{2} \left(\frac{\partial P}{\partial y} \right)^2 \right\}. \quad (1)$$

The angles ϕ_a and ϕ_b represent the directions of the two AFM sublattice magnetizations, respectively, relative to the $+x$ axis in the x - y plane. This is illustrated in Fig. 1 where an AFM domain wall is schematically shown between domains labeled 1 and 2, respectively. m_a and m_b are dimensionless, normalized magnetizations and may vary with position y . They are given by the normalized thermal averages $m_{a/b} = \langle M_{a/b} \rangle / M$. M is the zero temperature saturation magnetization of the material and the thermal average is calculated via

$$\frac{\langle M_{a/b} \rangle}{M} \equiv \mathcal{L} \left(\frac{\mu \mathbf{H}_{a/b}^{eff} \cdot \mathbf{m}_{a/b}}{k_B T} \right),$$

where $\mathcal{L}(x) = \coth(x) - 1/x$ is the Langevin function and $\mathbf{H}_{a/b}^{eff} = -\partial F / \partial \mathbf{M}_{a/b}$ is the effective magnetic field felt by the sublattice magnetizations. $\mu = 5\mu_B$ is the magnetic moment in the AFM, k_B is Boltzmann's constant, and T is temperature.

The first term in the integrand of Eq. (1) is the uniaxial (x axis) anisotropy energy density, with an anisotropy constant given by a second-order Taylor expansion with respect to P , namely, $K + kP^2$. A term linear in P is not allowed by the symmetry of BiFeO₃.¹³ A possible explanation for the phenomenological magnetoelectric coupling term with strength k is that a change in the electric polarization P gives rise to a Stark splitting of electron energy levels, which in turn leads to a change in the spin-orbit coupling giving rise to magnetic anisotropy.^{13,14}

The second term in the integrand of Eq. (1) is the Zeeman energy density with field applied along the x axis with strength b . The third term describes the AFM exchange between the sublattices with $J > 0$. The fourth term is the stiffness of the AFM magnetization and favors a wider domain wall. Again, the stiffness constant is given by a Taylor ex-

pansion with respect to P , $C + cP^2$. A physical mechanism behind this phenomenological magnetoelectric coupling term with strength c , is that a change in the FE polarization may alter the distance between AFM ions and therefore change the effective exchange and stiffness constants.^{13,15} The effect of P on the exchange constant J is ignored here as it does not result in domain-wall pinning.

The fifth term in Eq. (1) is the Dzyaloshinskii-Moriya energy density with strength D . It results in a very slight canting of the AFM sublattices by an angle of 0.14° ,¹⁶ resulting in a weak ferromagnetic moment in the $\pm y$ direction in domain 1 and 2, respectively (see Fig. 1), as will be discussed below. Here we assume that D has no dependence on P . The last line of Eq. (1) gives the free-energy density of the FE with Landau constants α and β , and stiffness constant κ . To include the effect of temperature, we assume that $\alpha = A(T_c^p - T)$, where A is a constant and $T_c^p = 1123$ K is the ferroelectric Curie temperature.¹³

Before examining bias, the effect of the magnetoelectric coupling (with strength given by k and c) on the domain walls in the isolated BiFeO₃ will be studied. The domain-wall configurations can be found numerically by converting the integral in Eq. (1) to a finite elements expression, $\int dy \rightarrow \Delta \sum_i$. Δ is the spacing between elements i and must be small enough that the domain walls can be resolved. The iteration algorithms for the magnetization angles are found by making $\frac{\delta F}{\delta \phi_{a/b,i}} = 0$ and then rearranging for $\phi_{a/b,i}$ to get an expression for the $n+1$ iteration of the form $\phi_{a/b,i}^{n+1} = f(\phi_{a/b,i}^n, m_{a/b,i}^n, P_i^n)$, where f is an analytic function. The same method cannot be used for P_i since the resulting expression only converges for $\Delta > \sqrt{(2\kappa/\alpha)}$ which is the FE wall width. Instead, we use a forward time central space algorithm

$$P_i^{n+1} = P_i^n - \frac{\epsilon}{\nu} \frac{\delta F}{\delta P_i^n},$$

where ϵ is the size of the “time” step and ν is the damping constant. This algorithm converges for $\frac{\kappa \epsilon}{\nu \Delta^2} < \frac{1}{2}$. Finally, the algorithm for $m_{a/b}$ is given simply by

$$m_{a/b,i}^{n+1} = m_{a/b,i}^n \cos^2 \xi + \sin^2 \xi \mathcal{L} \left(\frac{\mu \mathbf{H}_{a/b,i}^{eff,n} \cdot \mathbf{m}_{a/b,i}^n}{k_B T} \right),$$

where the angle ξ is chosen at random to ensure convergence. In general, choosing ξ close to zero made convergence slower but more likely.

As the starting point for iteration, the known analytic results for AFM and FE domain walls are used, found when magnetoelectric coupling is ignored and the integral in Eq. (1) is taken over an infinite extent

$$\phi_a(y) = 2 \tan^{-1}(e^{\sqrt{2K/C}(y-y_0)}),$$

$$\phi_b(y) = -2 \tan^{-1}(e^{-\sqrt{2K/C}(y-y_0)}),$$

$$P(y) = \sqrt{\frac{\alpha}{\beta}} \tanh\left(\sqrt{\frac{\alpha}{2\kappa}}(y - y_0)\right),$$

where y_0 is the position of the centre of each wall. With no demagnetizing or depolarizing energy included, the domain walls represent a metastable state for the system so the iteration must start sufficiently close to the solution to ensure convergence. It is assumed that there are two AFM and two FE domain walls to make use of periodic boundary conditions.

When $c > 0$ and/or $k > 0$, the AFM and FE domain walls are *pinned* to one another through magnetoelectric coupling. This is because in the vicinity of a FE domain wall $P \rightarrow 0$ and therefore the effective anisotropy and stiffness constants are locally weaker, making it a favorable place for AFM domain walls to be positioned. Conversely, when $c < 0$ and/or $k < 0$, the domain walls repel and the centre of the AFM domains, where the magnetizations are best aligned, coincide with the FE walls. This suggests that for known multiferroic systems where the domain walls coincide, the magnetoelectric coupling is positive within our scheme.

The y component of the magnetic moment of BiFeO₃, $m_i^y = m_{a,i} \sin \phi_{a,i} + m_{b,i} \sin \phi_{b,i}$, is plotted as a function of position $y = i\Delta$ in Fig. 2(a). The material parameters used are given in the figure caption. It is seen that the DM interaction gives rise to a weak moment in the two domains in $\pm y$ direction, respectively. The domain walls are located at $y = 50$ and 150 nm. Since domain 1 and domain 2 occupy equal volumes, there is not a net moment produced in the y direction.

However, there is also a moment in the AFM domain walls in the $\pm x$ direction, depending on the chirality of the wall. If within the AFM domain wall ϕ_a passes through $\pi/2$ then the weak DM moment is in the $+x$ while if instead ϕ_a passes through $-\pi/2$ then the weak moment is along $-x$. It is assumed from now on that the two AFM domain walls have opposite chirality (ϕ_a passes through $\pi/2$ in both walls) so that a net moment is produced in the $+x$ direction ($\sum_i m_i^x \neq 0$), as illustrated in Fig. 2(b) where $m_i^x = m_{a,i} \cos \phi_{a,i} + m_{b,i} \cos \phi_{b,i}$ is plotted as a function of position $y = i\Delta$. Although the net moment averaged across the whole 200 nm is quite small (under 0.1% of M), this is still large enough to give a bias, as will be shown numerically in the next section. A crude estimate of the effective exchange field felt by a FM due to this moment at zero temperature is given by $b_{ex} \sim 0.001 \times J_{int}/M_f$, where M_f is the magnetization of the FM and J_{int} is the exchange interaction across the FM/AFM interface. We estimate $J_{int} \sim 4 \times 10^6$ J/m³ and $M_f \sim 1.44 \times 10^6$ A/m for Co giving $b_{ex} \sim 0.003$ T ($H_{ex} = 30$ Oe).

III. EXCHANGE BIAS

To calculate exchange bias, a FM contribution is added to the 1D free-energy density [Eq. (1)]

$$F = \int dy \left\{ K_f \sin^2 \theta_f + \frac{1}{2} C_f \left(\frac{\partial \theta_f}{\partial y} \right)^2 - b M_f \cos \theta_f - J_{int} [\cos \theta_f (m_a \cos \phi_a + m_b \cos \phi_b) + \sin \theta_f (m_a \sin \phi_a + m_b \sin \phi_b)] \right\}. \quad (2)$$

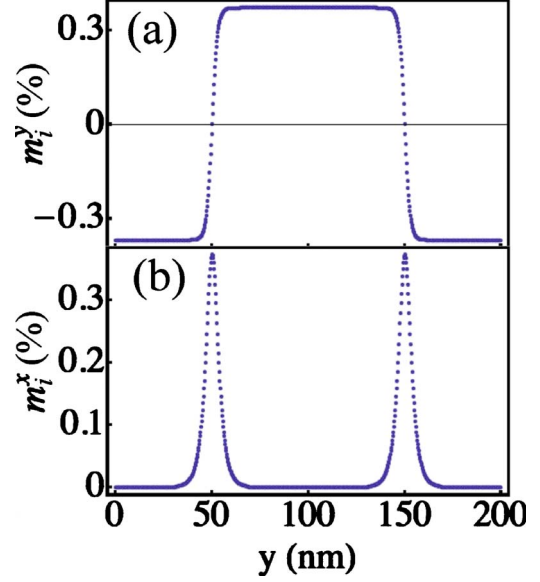


FIG. 2. (Color online) The normalized magnetic moment of BiFeO₃ in the (a) y direction ($m_i^y = m_{a,i} \sin \phi_{a,i} + m_{b,i} \sin \phi_{b,i}$) and (b) x direction ($m_i^x = m_{a,i} \cos \phi_{a,i} + m_{b,i} \cos \phi_{b,i}$) as a function of position $y = i\Delta$. A net moment is produced in the $+x$ direction when the two domain walls at $y = 50$ and 150 nm have opposite chirality. $\Delta = 0.25$ nm and $T = 300$ K. For BiFeO₃, $J = 4.3 \times 10^8$ J/m³, found by considering that the Néel temperature $T_N \sim 650$ K (Ref. 13), and $C = 107$ pJ/m. The magnetization is found by considering that each Fe ion has a moment $5\mu_B$ in a unit cell roughly $(0.4 \text{ nm})^3$ in volume (Ref. 17) giving $\mu_0 M = 0.94$ T. $K \sim 6.6$ MJ/m³ according to Ref. 18. It is calculated that $D \sim 2$ MJ/m³ in order for a canting angle $\chi = 0.14^\circ$ to be produced in the domains, which is consistent with a net moment of $0.012\mu_B$ measured per Fe (Ref. 16). The Landau parameters are taken to be $\alpha = 9.8 \times 10^5 (T - 1123)$ C⁻² m² N, $\beta = 2.6 \times 10^9$ C⁻⁴ m⁶ N (Ref. 19) and $\kappa = 6 \times 10^{-12}$ C⁻² m⁴ N (Ref. 20), which are within an order of magnitude of the parameters used in Ref. 12. The magnetoelectric coupling is assumed small; $cP^2 = 0.01C$ and $kP^2 = 0.01K$.

The FM magnetization is assumed to lie in the x - y plane and the angle it makes with the $+x$ direction is given by θ_f . The first term in Eq. (2) is the anisotropy (with constant K_f) favoring alignment along the x axis. The second term is the stiffness energy with constant C_f and the third is the Zeeman energy. The magnetization M_f is assumed constant since the ordering temperature is typically much larger than the AFM Néel temperature [$T_N \sim 650$ K for BiFeO₃ (Ref. 13) whereas the Curie temperature for Co, for example, is 1388 K (Ref. 21)]. The last term in Eq. (2) is the exchange coupling between the FM and the AFM across the x - y plane.

The numerical calculations in Sec. II can be repeated with the addition of these energies to find $\phi_{a/b}$, $m_{a/b}$, P , and θ_f at each finite element site i . The iteration algorithm for $\theta_{f,i}$ is found by rearranging $\frac{\delta F}{\delta \theta_{f,i}} = 0$. Two different solutions are obtained corresponding to local energy minima depending on whether iteration is begun from $\theta_{f,i} = 0$ or π . Making $J_{int} = 0$, these two solutions have equal energy when $b = 0$. In other words, a double well exists with symmetry that can be broken by an applied field. However, when $J_{int} \neq 0$, the two minima have different energies at zero field due to interac-

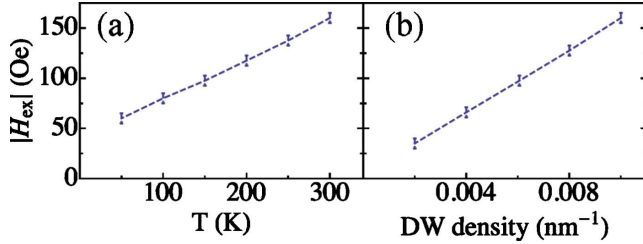


FIG. 3. (Color online) Exchange bias in a model Co/BiFeO₃ system as a function of (a) temperature and (b) domain-wall density. Conservative numerical error bars are drawn, as are dashed lines joining the points to highlight the trends. The parameters used for the numerical simulation are given in the caption of Fig. 2 and in the text. In panel (a), the domain-wall density is 0.01 nm⁻¹ and in panel (b) $T=300$ K.

tion with the net moment in the AFM. The strength of the exchange bias can be calculated by finding the applied field, $b=b_{ex}$, necessary for the two solutions with $\theta_{f,i} \sim 0$ and π to have equal energy.²²

The material parameters for BiFeO₃ are derived from experiment and are listed in the caption of Fig. 2. For the FM the values for Co are assumed: $M_f=1.44 \times 10^6$ A/m, $K_f=0.53$ MJ/m³, and $C_f=10.3$ pJ/m.²³ The only free parameter is the interface coupling between the FM and the AFM. It is assumed to be 5% of the AFM exchange coupling ($J_{int}=0.05J$) since this gives exchange bias of the correct order of magnitude. This seems like a reasonable assumption as it means the interface coupling is less than that inside either material. Experiment suggests that in fact J_{int} decreases as a function of temperature⁵ since the coercivity of a CoFe film on BiFeO₃ decreases. However, J_{int} is made constant so as to isolate the effect of temperature and domain-wall density on bias.

In Fig. 3(a) the magnitude of the exchange bias $|H_{ex}| = 10^4 \times |b_{ex}|$ is plotted as a function of temperature for a 200 nm sample (domain wall density is 0.01 nm⁻¹). Extrapolating to $T=0$, $|H_{ex}| \sim 40$ Oe, which matches closely to the estimate $|H_{ex}| \sim 30$ Oe calculated from the net moment in the isolated AFM. The bias increases with increasing temperature if J_{int} is constant. Considering that J_{int} decreases with T , as already mentioned, it can be understood why bias stays roughly constant with temperature, as seen in experiment (see Fig. 3 of Ref. 5). The bias increases in Fig. 3(a) because the magnetization in the antiferromagnet (m_{af}) decreases. At first, this may seem counterintuitive since the net moment Σm_i^x would also be expected to decrease leading to a smaller bias at higher temperatures. However, as the magnetization decreases, the exchange interaction between the FM and the AFM (which varies as m_{af}) begins to dominate the other AFM free-energy contributions [which vary as m_{af}^2 , see Eq. (1)]. Hence the net moment in the AFM is enhanced and the effective field felt by the FM increases.

In fact, the interface exchange characterized by J_{int} dominates over the DM interaction at all temperatures. For this reason it is not strictly correct to refer to a pinned net

moment in the AFM domain walls when the BiFeO₃ is attached to the FM. The magnetization in the domain walls will align along $\pm x$ according to the direction of the FM since the interface exchange dominates. In the $+x$ direction this alignment acts with the DM interaction and in the $-x$ direction the alignment acts against the DM interaction. This causes the two solutions with $\theta_{f,i} \sim 0$ and π , respectively, to have unequal energies and results in exchange bias.

In Fig. 3(b) the magnitude of the bias at $T=300$ K is plotted as a function of AFM domain wall density (the inverse of the distance between AFM walls). The same linear relationship is observed as is seen in experiment (see Fig. 2 of Ref. 5). The plot extrapolates back to the origin suggesting that there is no bias without pinned AFM domain walls present.

The fact that no training effect is seen in one experiment² can be explained qualitatively. In traditional FM/AFM exchange bias systems, training can be modeled using a domain state model.²⁴ In this model, the cycling of a magnetic field that can reverse the FM magnetization also causes slight rearrangement of the AFM domain structure through thermally assisted processes. Hence, each hysteresis loop shows a smaller exchange bias than the last as the AFM slowly rearranges to reduce all competing interactions. In the phenomenological model presented here, the AFM domain walls are pinned by the FE domain walls and hence less of a training effect may be expected. Future work may examine the size of this pinning potential to see how robust it is to thermal processes under different field sweep rates. The present model cannot examine this since there is no mechanism for the system to escape a metastable minimum through thermal processes.

IV. CONCLUSION

In summary, attraction and repulsion of antiferromagnetic and ferroelectric domain walls have been demonstrated in a 1D phenomenological model for BiFeO₃. In addition, exchange bias has been predicted in a Co/BiFeO₃ bilayer. The bias is due to two main features: the existence of AFM domain walls that are pinned by FE domain walls in the BiFeO₃, together with a net moment in the domain walls due to Dzyaloshinskii-Moriya interaction. For reasonable estimates of the exchange coupling between Co and BiFeO₃, the exchange bias is approximately 150 Oe at room temperature and for domain-wall density of 0.01 nm⁻¹. This value agrees well with experimental results for Co_{0.9}Fe_{0.1}/BiFeO₃ bilayers containing 109° FE domain walls.⁵

The main drawback of this theory is that it does not explain why only 109° FE domain walls pin the AFM domain walls, and not 180° or 71° FE domain walls. A full three-dimensional microscopic model is needed to investigate why this is so. Moreover, as mentioned earlier, only if the neighboring AFM domain walls have opposite chirality is a net moment produced. It does not result from field cooling since the BiFeO₃ is grown before the FM is deposited (in an

applied field) and is not heated.⁵ Hence it is an open question as to why the domain walls arrange with chirality such that a net moment is produced. It is possible that neighboring domain walls in a 1D model are most often part of the same wall in a two-dimensional picture and therefore necessarily have identical moments. This idea needs to be explored in future work.

ACKNOWLEDGMENTS

Support is acknowledged from the Australian Research Council. R. L. Stamps is thanked for help with the numerical routines and P. J. Metaxas for critically reading the manuscript.

*livesey@physics.uwa.edu.au

- ¹J. Dho, X. Qi, H. Kim, J. L. MacManus-Driscoll, and M. G. Blamire, *Adv. Mater.* **18**, 1445 (2006).
- ²H. Béa, M. Bibes, S. Cherifi, F. Nolting, B. Warot-Fonrose, S. Fusil, G. Herranz, C. Deranlot, E. Jacquet, K. Bouzehouane, and A. Barthélémy, *Appl. Phys. Lett.* **89**, 242114 (2006).
- ³Y.-H. Chu, L. W. Martin, M. B. Holcomb, M. Gajek, S.-J. Han, Q. He, N. Balke, C.-H. Yang, D. Lee, W. Hu, Q. Zhan, P.-L. Yang, A. Fraile-Rodriguez, A. Scholl, S. X. Wang, and R. Ramesh, *Nature Mater.* **7**, 478 (2008).
- ⁴M. Bibes and A. Barthélémy, *Nature Mater.* **7**, 425 (2008).
- ⁵L. W. Martin, Y.-H. Chu, M. B. Holcomb, M. Huijben, P. Yu, S.-J. Han, D. Lee, S. X. Wang, and R. Ramesh, *Nano Lett.* **8**, 2050 (2008).
- ⁶M. Fiebig, Th. Lottermoser, D. Fröhlich, A. V. Goltsev, and R. V. Pisarev, *Nature (London)* **419**, 818 (2002).
- ⁷I. E. Dzyaloshinskii, *J. Phys. Chem. Solids* **4**, 241 (1958).
- ⁸T. Moriya, *Phys. Rev.* **120**, 91 (1960).
- ⁹M. Bode, E. Y. Vedmedenko, K. von Bergmann, A. Kubetzka, P. Ferriani, S. Heinze, and R. Wiesendanger, *Nature Mater.* **5**, 477 (2006).
- ¹⁰S. Dong, K. Yamauchi, S. Yunoki, R. Yu, S. Liang, A. Moreo, J.-M. Liu, S. Picozzi, and E. Dagotto, *Phys. Rev. Lett.* **103**, 127201 (2009).
- ¹¹M. Daraktchiev, G. Catalan, and J. F. Scott, *Ferroelectrics* **375**, 122 (2008).
- ¹²M. Daraktchiev, G. Catalan, and J. F. Scott, *Phys. Rev. B* **81**, 224118 (2010).
- ¹³G. A. Smolenskiĭ and I. E. Chupis, *Sov. Phys. Usp.* **25**, 475 (1982).
- ¹⁴G. T. Rado, *Phys. Rev. Lett.* **6**, 609 (1961).
- ¹⁵K. L. Livesey and R. L. Stamps, *Phys. Rev. B* **81**, 094405 (2010).
- ¹⁶H. Béa, M. Bibes, S. Petit, J. Kreisel, and A. Barthélémy, *Philos. Mag. Lett.* **87**, 165 (2007).
- ¹⁷J. Wang, J. B. Neaton, H. Zheng, V. Nagarajan, S. B. Ogale, B. Liu, D. Viehland, V. Vaithyanathan, D. G. Schlom, U. V. Waghmare, N. A. Spaldin, K. M. Rabe, M. Wuttig, and R. Ramesh, *Science* **299**, 1719 (2003).
- ¹⁸F. Bai, J. Wang, M. Wuttig, J.-F. Li, N. Wang, A. P. Pyatakov, A. K. Zvezdin, L. E. Cross, and D. Viehland, *Appl. Phys. Lett.* **86**, 032511 (2005).
- ¹⁹J. X. Zhang, Y. L. Li, Y. Wang, Z. K. Liu, L. Q. Chen, Y. H. Chu, F. Zavaliche, and R. Ramesh, *J. Appl. Phys.* **101**, 114105 (2007).
- ²⁰J. X. Zhang, Y. L. Li, S. Choudhury, L. Q. Chen, Y. H. Chu, F. Zavaliche, M. P. Cruz, R. Ramesh, and Q. X. Jia, *J. Appl. Phys.* **103**, 094111 (2008).
- ²¹C. Kittel, *Introduction to Solid State Physics*, 7th ed. (Wiley, New York, 1996), p. 445.
- ²²There is no mechanism in our model for the system to escape from one energy well to another via thermal fluctuations. Therefore, a hysteresis loop obtained through this method has little physical meaning and a better way to estimate the bias is by finding the field that makes the two energy minima equal.
- ²³R. Skomski and J. M. D. Coey, *Permanent Magnetism* (Institute of Physics, Bristol, 1999).
- ²⁴U. Nowak, K. D. Usadel, J. Keller, P. Miltényi, B. Beschoten, and G. Güntherodt, *Phys. Rev. B* **66**, 014430 (2002).